Superlinearly scalable noise robustness of redundant coupled dynamical systems

Vivek Kohar,[1,*] Behnam Kia,[1] John F. Lindner,[2] and William L. Ditto[1]
[1]*Department of Physics, North Carolina State University, Raleigh, North Carolina 27695-8202, USA*
[2]*Physics Department, The College of Wooster, Wooster, Ohio 44691, USA*
(Received 11 November 2015; published 11 March 2016)

We illustrate through theory and numerical simulations that redundant coupled dynamical systems can be extremely robust against local noise in comparison to uncoupled dynamical systems evolving in the same noisy environment. Previous studies have shown that the noise robustness of redundant coupled dynamical systems is linearly scalable and deviations due to noise can be minimized by increasing the number of coupled units. Here, we demonstrate that the noise robustness can actually be scaled superlinearly if some conditions are met and very high noise robustness can be realized with very few coupled units. We discuss these conditions and show that this superlinear scalability depends on the nonlinearity of the individual dynamical units. The phenomenon is demonstrated in discrete as well as continuous dynamical systems. This superlinear scalability not only provides us an opportunity to exploit the nonlinearity of physical systems without being bogged down by noise but may also help us in understanding the functional role of coupled redundancy found in many biological systems. Moreover, engineers can exploit superlinear noise suppression by starting a coupled system near (not necessarily at) the appropriate initial condition.

DOI: 10.1103/PhysRevE.93.032213

I. INTRODUCTION

Dynamical systems are used as prototypical models for many natural systems and have inspired a large number of engineering applications [1–11]. Over the past few decades, the shrinking of devices and signals in engineering applications has meant that the effects of nonlinearities and the intrinsic noise of systems can no longer be neglected. Similarly, studies on biological systems indicate that they are inherently nonlinear and operate in noisy environments. Nonlinear dynamical systems are very sensitive to small changes, and their interaction with noise has been extensively studied [12–16]. Still, the interaction of biological systems with intrinsic and extrinsic noise is yet to be fully understood. The individual dynamical units in these systems do not function in isolation and are generally coupled with each other through one or more variables. Theoretical and experimental studies on such coupled nonlinear dynamical systems have uncovered interesting phenomena like synchronization [17,18].

The role of coupled dynamics as a noise reduction mechanism has been studied recently [8,19–24]. Coupling between redundant nonlinear dynamical systems can enhance the noise robustness and has been shown to play an important part in neural learning and decision making [21]. It was pointed out that if the dynamical systems are nonlinear then using redundancy and linear averaging may not yield a meaningful signal [20,25]. In such cases, coupling of dynamical units can result in linearly scalable reduction of deviations caused by local noise [22,23]. It was shown that globally coupled maps (GCM) initialized to the same initial condition and evolving in the presence of local noise suffer lower deviations from noise free evolution as compared to isolated maps evolving in the same environment. Thus such redundant coupled systems act as averaging filters and this phenomenon can be utilized to enhance the noise robustness of dynamical systems without use of any additional averaging hardware. A practical application of this method was demonstrated in chaos computing [8,10,26] where the coupled units had lower error rates as compared to individual units for a given noise floor [23,27].

In this paper, we show that superlinearly scalable noise robustness can be realized in redundant coupled dynamical systems. Such high noise robustness is observed near the "superstable" points where the first derivative of the function describing the evolution rule vanishes. Superstability has been previously studied in periodic orbits [28–31] and limit cycles [32,33] and been found useful in applications [34,35]. The previous studies focused on the role of bifurcation parameters and the existence of superstable orbits for specific bifurcation parameters. The superstable orbits also exist for bifurcation parameters at which the system is chaotic, and thus high noise robustness can be obtained even in chaotic systems. Motivated by this, we study the role of initial conditions and iteration number or evolution time in superstability. We find that the effects of noise are not only lower for these combinations of initial conditions and evolution time but the use of coupled redundancy results in superlinear reduction of the effects of the noise, which makes these configurations ideally suited for applications.

In the next section, we describe the general principle of this mechanism and illustrate it with explicit numerical simulations in coupled map lattices. In the penultimate section, we discuss the mechanism in flows modeled by coupled differential equations and summarize the results in the last section.

II. MAPS

For simplicity and easier quantification, we first describe the working principle in the case of one-dimensional maps. Let us consider a prototypical dynamical system given by

$$x_{i+1} = f(x_i), \tag{1}$$

where x is the state variable, i the iteration number, and $f(x)$ is the function describing the evolution rule. We assume

*vkohar@ncsu.edu

that this map evolves in the presence of local additive noise with variance σ_δ^2 such that the initial condition of the map is modified as $x^0 \to x^0 + \delta_0$ and a noise term δ_i is added at every subsequent iteration i. We denote the deviation after iteration i of maps evolving in the presence of noise from a noiseless map by

$$\Delta_i = f(\cdots f(f(x_0 + \delta_0) + \delta_1) \cdots + \delta_{i-1}) - f(\cdots f(f(x_0))). \quad (2)$$

The Taylor series expansion of $f(x)$ about x_0 after first iteration gives

$$f(x_0 + \delta_0) = f(x_0) + \left\{ \frac{\lambda_{x_0}^1 \delta_0}{1!} + \cdots + \frac{\lambda_{x_0}^n \delta_0^n}{n!} + \cdots \right\}, \quad (3)$$

where $\lambda_{x_0}^n$ is nth derivative of $f(x)$ evaluated at x_0. The second term in Eq. (3) represents the deviation due to noise at first iteration, Δ_1, of a map evolving in a noisy environment from a map evolving in a noiseless environment. The second and higher order terms can be neglected if noise is low. For linear dynamical systems $f(x)$ is a first order polynomial, and consequently $\lambda_{x_0}^1$ is constant and $\lambda_{x_0}^n = 0$ for $n \geqslant 2$ and so Δ depends only on δ_0. In contrast, the Taylor series expansion of $f(x)$ is a higher order polynomial in nonlinear systems and $\lambda_{x_0}^1$ has terms containing x_0. Thus Δ depends not only on δ_0, but also on x_0. Δ is minimum when $|\lambda_x|$ is minimum where $|\lambda_x|$ is the absolute value of λ evaluated at x. So the deviations from the noise free behavior depend on the specific initial condition of the system and some initial conditions are more robust against noise as compared to others.

Now we consider a generalized globally coupled map lattice (CML) [36] of N maps coupled through mean field coupling. The CML can be written as

$$x_{i+1}^n = (1-c) f\left(x_i^n\right) + \frac{c}{(N-1)} \sum_{l,l\neq n}^{N} f\left(x_i^l\right), \quad (4)$$

where x_i^n is the state of the nth node at the ith iteration and c is the coupling strength. It was shown in [22] that maximum noise robustness is obtained when $c = (N-1)/N$. We will use this value of coupling strength for the rest of the discussion. Under this assumption Eq. (4) becomes

$$x_{i+1}^n = \frac{1}{N} f\left(x_i^n\right) + \frac{1}{N}\left(\sum_{l,l\neq n}^{N} f\left(x_i^n\right)\right) = \frac{1}{N}\sum_{l=1}^{N} f\left(x_i^l\right). \quad (5)$$

We evolve the CML in the presence of a statistically independent but identically distributed Gaussian white noise with zero mean and standard deviation σ_δ. Further, all the nodes of the CML are initialized with the same initial condition such that $x_0^n = x_0$. This allows us to study the role of redundancy in reducing the effects of noise. The presence of noise modifies the initial conditions of individual nodes of the CML as given by Eq. (6). As the noise is local, identically distributed and statistically independent, the instantaneous noise at each node is different, such that

$$x_0{}^n \to x_0^n + \delta_0^n = x_0 + \delta_0^n. \quad (6)$$

The state of the nth node at first iteration is given by

$$x_1^n = f\left(x_0 + \delta_0^n\right) + \frac{1}{N}\sum_{l\neq n} f\left(x_0 + \delta_0^l\right). \quad (7)$$

Using the Taylor expansion of the above equation around x_0 as described in Eq. (3) and neglecting the second and higher order terms, we obtain

$$x_1^n = f(x_0) + \frac{\lambda_{x_0}^1}{1!}\left(\frac{1}{N}\sum_{l}^{N} \delta_0^l\right). \quad (8)$$

The first term in Eq. (8) is the evolution of a noise free map and the effects of noise are contained in the second term. We call this deviation in the map's state after first iteration Δ_1^{CML}. For statistical significance, we calculate Δ_1^{CML} for many different realizations of noise terms and then calculate the variance of these deviations, $\sigma_{\Delta_1^{CML}}^2$. The instantaneous noise values are independent and identically distributed and so the total variance of these terms will be equal to $1/N$ times the variances of individual terms,

$$\sigma_{\Delta_1^{CML}}^2 = \sigma_\delta^2 \frac{\left(\lambda_{x_0}^1\right)^2}{N}. \quad (9)$$

We repeat the same process for an isolated map evolving in the same noisy environment. We neglect second and higher order terms in Eq. (3) and calculate the variance of deviations after first iteration which is given by

$$\sigma_{\Delta_1}^2 = \sigma_\delta^2 \left(\lambda_{x_0}^1\right)^2. \quad (10)$$

To compare the deviations due to noise in a CML and an isolated map, we define noise robustness as the ratio of variances of deviations in the CML and single map [22], namely

$$R = \frac{\sigma_\Delta^2}{\sigma_{\Delta^{CML}}^2}. \quad (11)$$

From Eqs. (9), (10), and (11), the noise robustness at first iteration, $R_1 = N$. So a CML consisting of N dynamical units lowers the variance of deviations due to noise by a factor of N after one iteration. At subsequent iterations, the deviations of maps will depend on the noise at $(i-1)$th iteration as well as Δ_{i-1}^n, that is, the deviation caused by noise in the preceding iterations.

In the case of chaotic systems, the deviations increase rapidly with iterations and the deviation due to noise at previous iterations quickly overshadows the noise term at the current iteration. Soon, the deviations are comparable to the size of the attractor and saturate afterwards. The number of iterations after which the deviations saturate depends on the noise level and the initial condition as different initial conditions have different sensitivity to noise. As a matter of fact, some of the initial conditions are superstable points, x_s, characterized by $\lambda_{x_s}^1 = 0$. Noise has little effect at x_s and the variance of deviations due to noise increases nonlinearly moving away from x_s. If any initial condition is mapped onto the superstable point x_s at $(i-1)$th iteration in the noiseless environment then it will be mapped to $x_s \pm \Delta_{i-1}$ in the noisy environment. As $\lambda_{i-1}^1 = 0$, the first order linearization will not be sufficient and higher order terms will have to be taken into consideration. Thus the difference Δ_{i-1} will evolve nonlinearly at the ith iteration and Δ_i will depend

on the nonlinearity of the map near the unstable fixed point. Similarly, the CML will be mapped to $x_s + \Delta_{i-1}^{CML}$ such that $\sigma^2_{\Delta_{i-1}} = N\sigma^2_{\Delta_{i-1}^{CML}}$. Again Δ_{i-1}^{CML} will evolve nonlinearly and thus the noise robustness at ith iteration depends on the nonlinearity of the map near the superstable point. Thus if $\lambda^1_{i-1} \sim 0$ for an initial condition x_0, the deviations due to noise will be minimum after ith iteration and the noise robustness will increase superlinearly with increase in number of coupled units. We call these configurations *super-robust* configurations as coupling a number of these redundant systems results in superlinear reduction of the effects of noise. For higher dimensional systems, manifold foliations can be complicated and one can identify the covariant Lyapunov vectors for an intrinsic decomposition of the tangent space [37,38].

We examine the above arguments in a simple one-dimensional quadratic map which is given by

$$x_{i+1} = 1 - a(x_i)^2. \tag{12}$$

This map is chaotic in the interval $x_i \in [-1,1]$ for $a = 2$. We simulate the map's evolution in a noiseless environment as well as in the presence of white noise with variance σ^2_δ. We iterate the map in noisy and noiseless environments for a fixed number of iterations and calculate the deviation of the state variable of the map evolving in the noisy environment from the value of the state variable of the map in a noiseless environment and call this deviation Δ as given by Eq. (2). We repeat this procedure, each time starting with the same initial condition, to obtain a large ensemble of deviations corresponding to different realizations of noise. Then we calculate the variance of these deviations, σ^2_Δ, for that particular initial condition. We again repeat the above procedure for various initial conditions and σ^2_Δ for different initial conditions as is shown in Fig. 1. We observe that different initial conditions have different sensitivities to noise. For the quadratic map, $df(x)/dx = \lambda^1 = -2ax$, which implies that $x = 0$ is a superstable point. Consequently, σ^2_Δ is minimum for $x = 0$ after first iteration. Similarly, for second iteration, we observe a minima at $x_0 = \pm 1/\sqrt{2}$. At first iteration both $\pm 1/\sqrt{2}$ will be mapped to zero, which is a superstable point. The minimum variance points for further iterations can be computed similarly. We observe that the overall deviations increase with the iteration number and the variance of deviations differs by four to six orders of magnitude for different initial conditions. Further, the number of initial conditions that have low deviations due to noise increases with the number of iterations. These initial conditions are not equally robust and the deviation, Δ_i, at an iteration i is dependent on the deviation due to noise at previous iterations, Δ_{i-1}.

We repeat the same procedure for a CML of quadratic maps with $N = 3$ and coupled in accordance with Eq. (5). Then we calculate noise robustness R for each initial condition by calculating the ratio of variance of the deviations in a single noisy map and noisy CML as shown in Fig. 2. We observe spikes in noise robustness around the specific superstable initial conditions identified above. As mentioned earlier, the deviations Δ depend on the noise strength σ_δ. We also examined how the robustness varies when the noise strength changes. The noise robustness around the superstable point $x_0 = 0.243$ is plotted in Fig. 3. We observe that higher noise robustness is obtained over a wider window around x_0

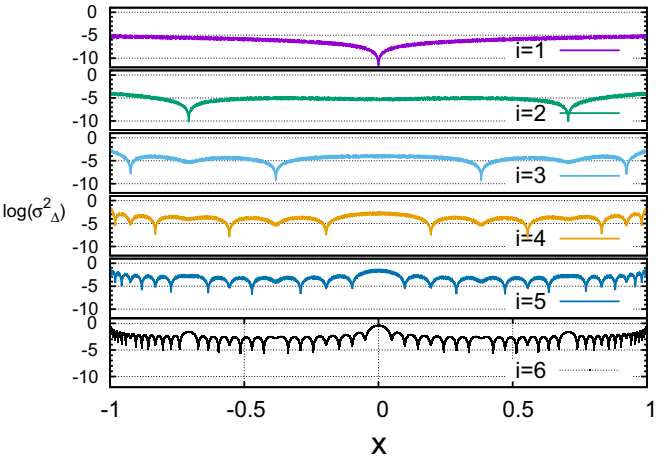

FIG. 1. Variance of deviations (log scale) of 10^4 simulations due to noise of variance $\sigma^2_\delta = 10^{-6}$ in a quadratic map for different initial conditions. Different colors show the variance for different iteration numbers.

for higher noise variance. When noise variance is higher, $x + \delta$ has a wider spread and thus the number of initial conditions which can be mapped to the super-robust value increases and consequently their noise robustness increases. Similarly, the initial conditions, which would have been mapped to super-robust value in the noise free case, may be mapped to nearby values and thus the maximum noise robustness value at the super-robust value decreases as the noise strength increases.

To study the scalability of noise robustness, we increased the number of nodes in the CML and observed how R varies with N. We found that typically $R \sim N$ but for super-robust initial conditions R increases superlinearly with N. Noise robustness for the quadratic map scaled with the number of node is plotted in Fig. 4.

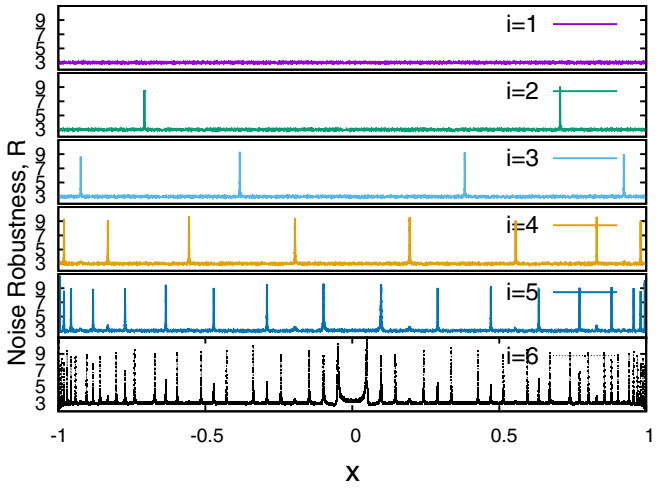

FIG. 2. Noise robustness for 10^4 simulations due to noise of variance $\sigma^2_\delta = 10^{-6}$ and $N = 3$ in a quadratic map for different initial conditions. Note that the superstable initial conditions result in spikes in noise robustness

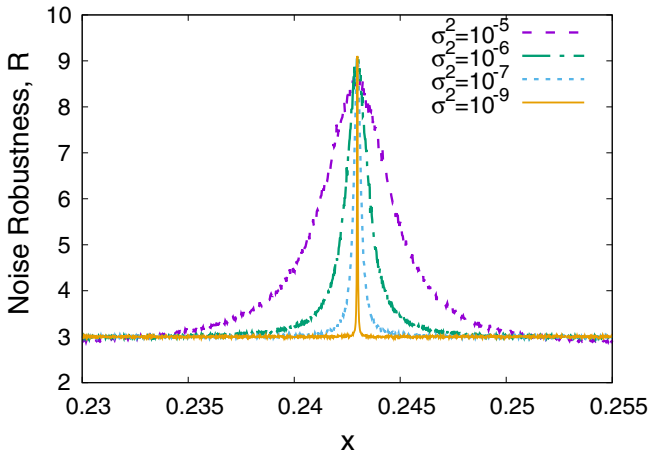

FIG. 3. Noise robustness R vs initial condition x_0 of a globally coupled CML of chaotic quadratic maps in presence of noise with varying variance σ_δ^2 after iteration number $i = 6$ near $x_0 = 0.243$. Higher noise robustness is obtained over a wider window around x_0 for higher noise variance.

To understand the scaling of R near the super-robust points, we measured R for varying N at the selected super-robust points as shown in Fig. 5. We found that R for the quadratic map scales as N^2. To verify the generality of our observations about the superlinear scaling of noise robustness for some specific initial conditions, we calculated the scaling for logistic as well as tent map. The logistic map has quadratic nonlinearity given by

$$x_{i+1} = r x_i (1 - x_i), \tag{13}$$

and the tent map is a piecewise linear map given by

$$x_{i+1} = f_\mu(x_i) = \begin{cases} \mu x_i & \text{for } x_i < \frac{1}{2}, \\ \mu(1 - x_i) & \text{for } \frac{1}{2} \leqslant x_i. \end{cases} \tag{14}$$

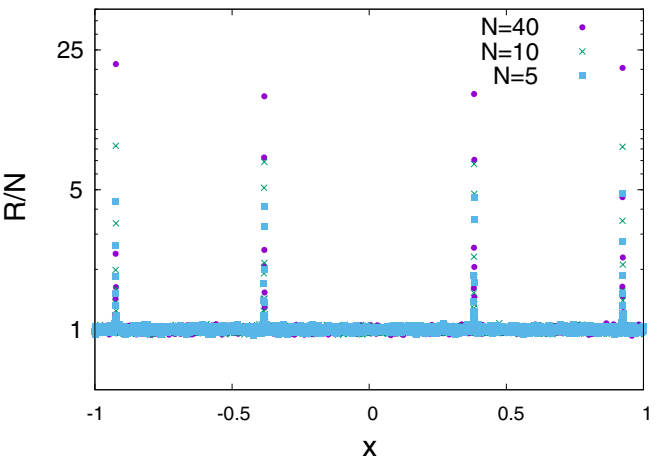

FIG. 4. Scaled noise robustness R/N vs initial condition x_0 of a globally coupled CML of chaotic quadratic maps in presence of noise with variance $\sigma_\delta^2 = 10^{-6}$ after iteration number $i = 3$. Noise robustness R is much larger than number of coupled units N for initial conditions near the superstable points. Increase in the number of nodes results in superlinear increase in R for super robust initial conditions and a linear increase for others.

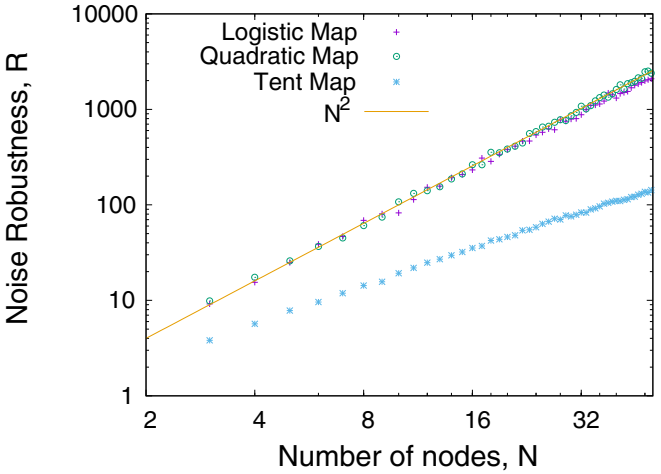

FIG. 5. Noise robustness R vs lattice size N of a globally coupled CML in presence of noise with variance $\sigma_\delta^2 = 10^{-6}$ for quadratic map for $x_0 = 0.243$ at $i = 6$, logistic map for $x_0 = 0.6913$ at $i = 3$, and tent map for $x_0 = 0.3725$ at $i = 3$.

Logistic map and tent map are in chaotic region for $r = 4$ and $\mu = 2$, respectively. For these values of parameters, we found that R for logistic map scales as N^2, whereas scaling exponent for the tent map is lower. These observations suggest that R also depends on the nonlinearity of the map. Quadratic and logistic maps have quadratic nonlinearities, whereas tent map is piecewise linear and so the scaling exponent for logistic and quadratic maps is higher than that of the tent map.

The above observations suggest that the super-noise robustness of superstable initial conditions is a generic phenomenon that can be observed in a wide variety of dynamical systems. The number of such initial conditions increases with increase in iteration number and after few iterations one can find a fairly large number of super-robust initial conditions. The upper limit on the number of iterations for which high noise robustness can be obtained is limited to the point where the deviations due to noise become comparable to the size of the attractor of the map.

III. FLOWS

Let us consider a coupled system consisting of N nodes where the nodes can be described by coupled ordinary differential equations in the form of a m-dimensional vector $\mathbf{x}^j$ where j $(1 \leqslant j \leqslant N)$ is the index of the node. In the coupled system, these nodes are coupled through one or more state variables with coupling strength c and coupling function $\mathbf{H}$. The dynamics of the uncoupled node is given by $\dot{\mathbf{x}}_j = \mathbf{F}(\mathbf{x}_j)$ and coupling topology is contained in the connectivity matrix $\mathbf{G}$ such that for the diffusive coupling $\sum_k G_{jk} = 0$. The coupled dynamics can now be written as

$$\dot{\mathbf{x}} = \mathbf{F}(\mathbf{x}) + c\mathbf{G} \otimes \mathbf{H}(\mathbf{x}), \tag{15}$$

where $\otimes$ denotes the direct product. Initially all nodes are initialized to the same initial condition on the attractor and they evolve in the presence of local additive white noise with noise variance σ_δ^2. The noise terms can then be considered as the perturbations of the synchronized state. The variational

equation of Eq. (15) can then be written in terms of Jacobian functions $D\mathbf{F}$ and $D\mathbf{H}$ as

$$\dot{\xi} = [\mathbf{1_N} \otimes D\mathbf{F} + c\mathbf{G} \otimes D\mathbf{H}]\xi, \tag{16}$$

where ξ_j are the variations of the jth node. Equation (16) can be rewritten in the black diagonalized form as [39]

$$\dot{\xi}_\mathbf{l} = [D\mathbf{F} + c\gamma_l D\mathbf{H}]\xi_\mathbf{l}, \tag{17}$$

where γ_l are eigenvalues of $\mathbf{G}$. One can evaluate the maximum Floquet or Lyapunov exponents and the covariant Lyapunov vectors of these equations for different γ_l which provide information about the evolution of the coupled system. Under optimal coupling, the perturbations due to noise can be averaged out in the coupled system and thus the overall deviations in the coupled system will be less than that of a single system. As the variational equation is nonlinear, the deviations due to perturbations will evolve nonlinearly and consequently the noise robustness varies superlinearly. Depending on the coupling topology, the deviations in some nodes may be affected more than others. Thus all nodes may be equally robust to noise or the noise robustness may vary among the nodes depending on their neighborhood [24].

Here, we consider the simple case of globally coupled oscillators such that noise robustness will be maximum and similar for all the nodes and one can select any node to measure the output. For this one must ensure that the coupling strength and topology are such that the synchronized state is stable and the nodes do not desynchronize due to noise. For diffusively coupled systems, $\gamma_0 = 0$ and thus $l = 0$ gives the variational equation for the synchronization manifold and other l's give the variational equations for the transverse modes. The conditions for the stability of synchronization can be easily identified using the master stability function approach [39]. Additionally, the basin stability should also be high as otherwise the noise in the system can destabilize it [40,41]. Under these conditions, the perturbations along the transverse modes will die out and the effect of perturbations along the synchronized state will depend on the Lyapunov exponent. If the synchronized state is chaotic, the Lyapunov exponent is positive and the deviations due to perturbations along the synchronization manifold will be magnified nonlinearly. For the coupled system, the average deviation of the synchronized state is less than the deviation of a single node. These deviations evolve nonlinearly along the synchronization manifold resulting in superlinear scaling of noise robustness of the coupled system.

We demonstrate the validity of the above arguments using numerical simulations of the mean field x-coupled Rössler oscillators [42] given by

$$\dot{x_j} = -y_j - z_j - c\sum_{k=1}^{N}(x_k - x_j), \tag{18}$$

$$\dot{y_j} = x_j + a_1 y_j, \tag{19}$$

$$\dot{z_j} = a_2 + z_j(x_j - a_3). \tag{20}$$

This oscillator is chaotic for the parameter values $a_1 = a_2 = 0.2$ and $a_3 = 7.0$. We initialize the nodes with an initial condition on the synchronized manifold and evolve the coupled as well as the uncoupled oscillators in noisy environment and measure their deviations from the noise free evolution. The noise terms are added to all three state variables x_j, y_j, z_j. The deviation is defined as the Euclidean norm of the difference in the state vector of noise free evolution and any one of the nodes of the coupled system. The noise robustness R and the variance of deviations σ^2_Δ of the isolated system for x state variable are shown in Fig. 6.

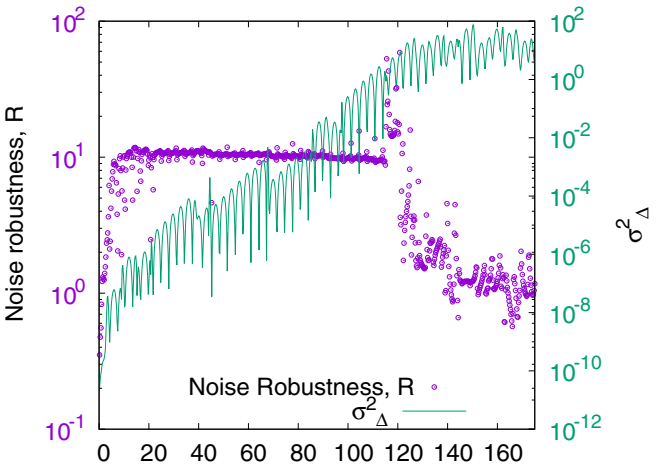

FIG. 6. Noise robustness R with time T of globally coupled Rössler oscillators in presence of noise $\sigma^2_\delta = 0.0004$, $N = 10$, and $c = 0.2$. The scale on right side corresponds to variance of deviations, σ^2_Δ, of the isolated map.

We observe that σ^2_Δ increases with time nonmonotonously and saturates as the deviations approach the size of the attractor. The deviations do not increase monotonically but instead exhibit maxima and minima on the time scale of the attractor. Further, the deviations increase slowly in the coupled system as evident from the rapid increase in the noise robustness, R, till it approaches N. Occasionally, there are bumps in noise robustness which are similar to the case of maps and correspond to the time when the σ^2_Δ is at a minima or the system is near a point in the trajectory where one of the

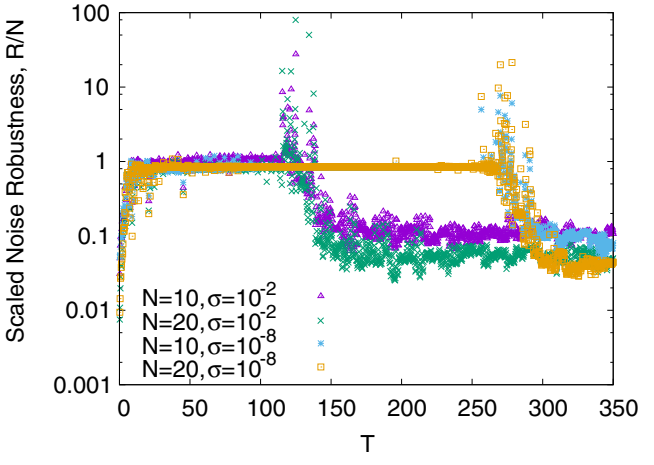

FIG. 7. Scaled noise robustness with time T of globally coupled Rössler oscillators in presence of noise of strength $\sigma^2_\delta = 10^{-4}$ for different number of coupled units. Also shown is the evolution of scaled R for different noise strengths.

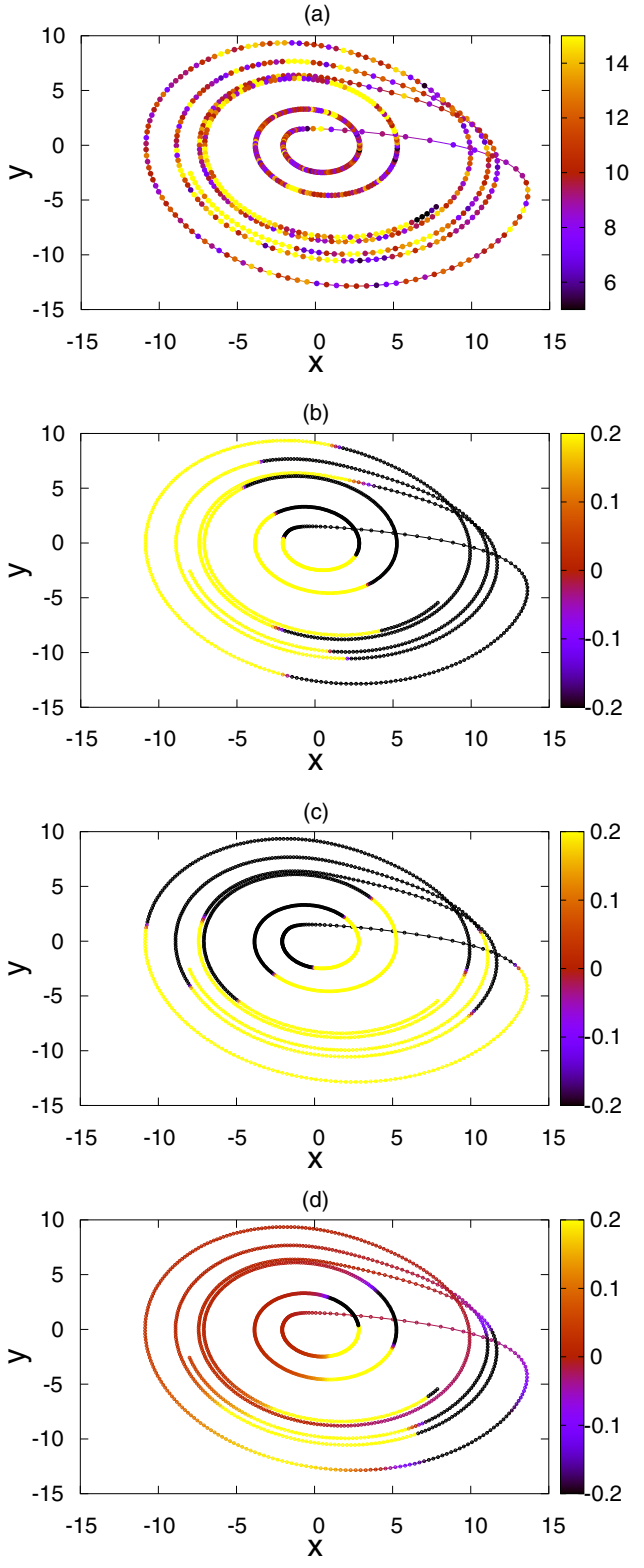

FIG. 8. (a) Noise robustness R for various initial conditions after time $T = 60$ for globally coupled Rössler oscillators in presence of noise of strength $\sigma_\delta = 1$, coupling strength $c = 0.2$, and $N = 10$. We observe that in some windows of initial conditions $R \gg 10$. For better visualization, we have used a threshold for R so that $R = 15$ for all $R > 15$. Color scale in (b),(c),(d) show $\dot{x}, \dot{y}, \dot{z}$ at $T = 60$ for a system starting at an initial condition given by x, y, z value. To highlight the region where $\dot{x}, \dot{y}, \dot{z} = 0$ we have used a threshold of ± 0.2.

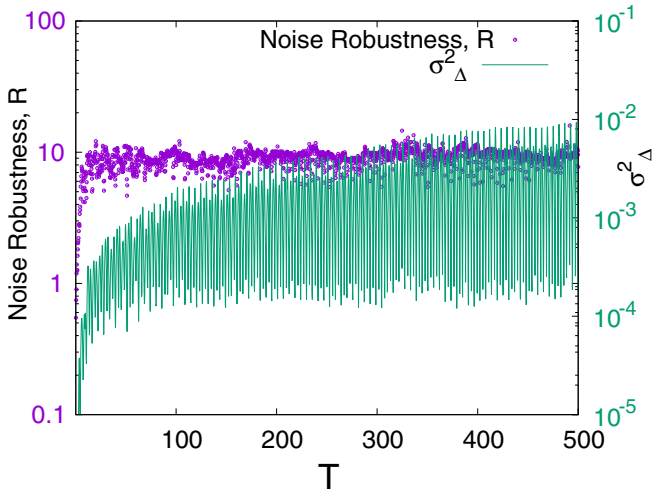

FIG. 9. Noise robustness R after time $T = 50$ of globally coupled Rössler oscillators in presence of noise $\sigma_\delta^2 = 0.0004$, $N = 10$, and $c = 0.2$. The scale on right side corresponds to variance of deviations, σ_Δ^2, of the isolated oscillator.

elements of $F(x)$ is close to zero. When the deviations due to noise are large enough, the nonlinear effects become dominant and we observe very high values of noise robustness (see Fig. 6 near $T \sim 120$). Soon afterwards, noise robustness drops to 1 as deviations in both coupled and isolated systems are of the order of the size of the attractor.

In Fig. 7, we scale the noise robustness with the number of coupled units in the coupled system. We observed that the superlinear increase in R for $\sigma_\delta = 0.01$ is achieved at approximately the same time ($T \sim 130$) for all $N = 5, 10, 20$. This is expected as the deviations start increasing nonlinearly in the isolated system near this time whereas such increase is suppressed in the coupled system. We plot the scaled R for another noise strength to verify this finding. We further verified that the phenomenon can be observed for a large window of coupling strengths. The upper limit of coupling strength c to which high noise robustness R can be obtained decreases with increase in the number of coupled nodes, N.

We studied the behavior for other initial conditions distributed over the synchronized attractor and the results are shown in Fig. 8. We observed that for a fixed evolution time, there are narrow bands of initial conditions for which very high R can be obtained.

To verify our arguments about the dependence of deviations on the Lyapunov exponents, we studied the noise robustness in limit cycle oscillators also. For $a_3 = 2.5$ in Eq. (20), the coupled Rössler system exhibits synchronized limit cycle dynamics. Noise robustness and variance of deviations in an uncoupled system are shown in Fig. 9. No sharp peaks were observed in noise robustness for this dynamics. This is in accordance with our previous arguments as the Lyapunov exponent for perturbations along the transverse modes is negative and zero along the synchronized manifold. Any perturbations are strongly damped in limit cycle oscillators and the overall deviations remain very low unless the parameter values are close to critical value corresponding to supersensitive cycles [16]. In Fig. 9, we observe that variance

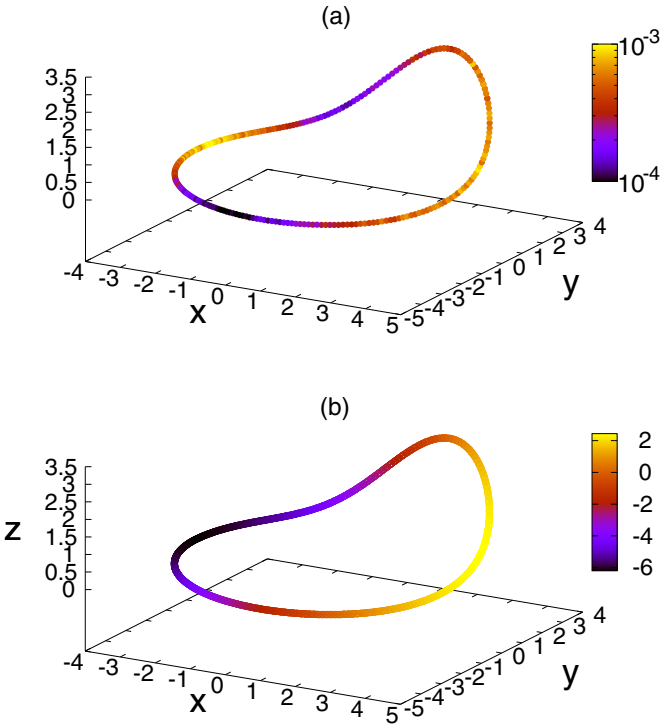

FIG. 10. Top panel shows the variance of deviations due to noise, σ^2_Δ, for globally coupled Rössler oscillators exhibiting a limit cycle in presence of noise of strength $\sigma^2_\delta = 4$, coupling strength $c = 1.0$, $N = 10$, and $T = 50$. The bottom panel shows the value of Jacobian evaluated on the attractor.

of deviations is less than 0.01 even after long evolution time and high noise strength. Thus the nonlinear effects are difficult to observe in limit cycle oscillators. Qualitatively similar behavior was observed for noise strengths varying from 10^{-6} to 10. Nonetheless, there are significant differences among the deviations in the initial conditions selected from the attractor. The variance of deviations after time $T = 50$ for different

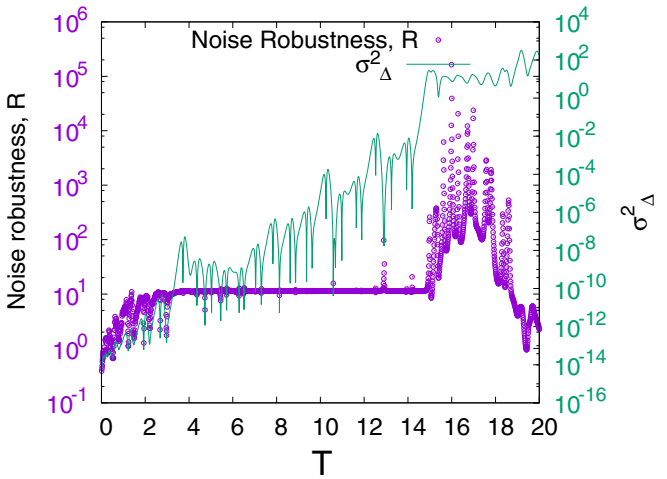

FIG. 11. Noise robustness R for globally coupled chaotic Lorenz oscillators in presence of noise with $\sigma_\delta = 0.1$, coupling strength $c = 0.1$, and $N = 10$.

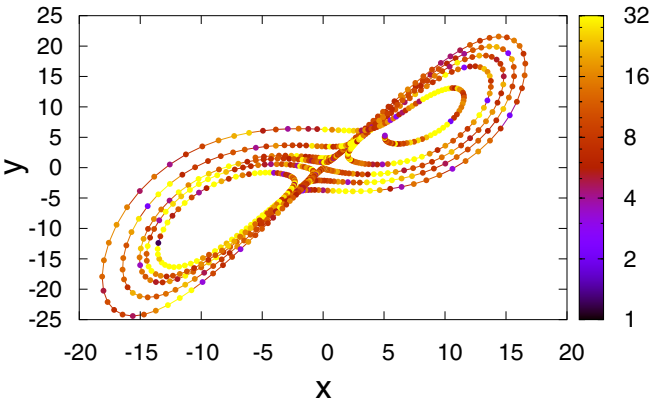

FIG. 12. Noise robustness R for different initial conditions at $T = 14$ for globally coupled Lorenz oscillators in presence of noise with $\sigma^2_\delta = 10^{-4}$, $N = 10$, and $c = 0.2$. For better appearance, R is thresholded at 32 such that if $R > 32$, we set $R = 32$.

initial conditions over the attractor is shown in Fig. 10. This difference in sensitivity of initial conditions shows that we can tune the initial conditions based on the evolution time to select the ones which are more stable against deviations. In the lower panel of Fig. 10, we plot the value of the Jacobian over the limit cycle which explains the different sensitivity of initial conditions to noise. The deviations are minimum when the Jacobian approaches zero.

We also studied the noise robustness of x-coupled Lorenz oscillators given by

$$\dot{x_j} = \gamma(y_j - x_j) - c\sum_{k=1}^{N}(x_k - x_j), \tag{21}$$

$$\dot{y_j} = x_j(\rho - z_j) - y_j, \tag{22}$$

$$\dot{z_j} = x_j y_j - \beta z_j, \tag{23}$$

where x, y, and z are state variables and the system is chaotic for $\gamma = 10$, $\beta = 8/3$, and $\rho = 28$. The evolution of a typical trajectory is shown in Fig. 11. Similar to Rössler oscillator, we observe sharp peaks in noise robustness. The peaks correspond to the points on the attractor where the effects of noise are minimum. The increase in R from $T \sim (15–18)$ results from the nonlinear amplification of deviations. As the deviations in CML are less than that of an isolated map, we get a significant increase in R. The noise robustness for various initial conditions selected from the Lorenz attractor after an evolution time $T = 14$ is shown in Fig. 12. We observe that there are many initial conditions for which high noise robustness is obtained.

IV. CONCLUSION

We have shown that coupling among redundant dynamical systems can enable them to function robustly in presence of noise and the noise robustness of a coupled system can scale superlinearly with the number of coupled units. Different initial conditions have different sensitivity to noise which further depends on the iteration number or the evolution time and noise strength. In the case of maps, selection of an appropriate

combination of the iteration number and the initial condition in optimally coupled maps can ensure very high robustness with few coupled units. The number of such super-robust initial conditions increases with each iteration and the window of high noise robustness widens as the noise levels increase. Similarly, higher noise robustness can be achieved in continuous time systems when the deviations due to noise are large. These large deviations can be a result of large noise intensity or long evolution time. The superlinear scaling of noise robustness can be easily observed in chaotic systems where the deviations due to noise are quickly magnified and thus redundant coupled systems can perform much better than a single system. The high robustness can be achieved only when the deviations due to noise are smaller than the size of the attractor of the dynamical system. This sets the limits on the iteration number or evolution time after which the system needs to be reset. For practical applications, one can choose evolution time or the initial condition to achieve superlinear scalability of noise robustness. Such super-robust configurations provide an opportunity to exploit the nonlinearity of physical systems without being bogged down by noise. Engineers may exploit superlinear noise suppression by starting a coupled system near (not necessarily at) the appropriate initial condition. This combination of initial condition and iteration number will provide three distinct advantages: (i) superstability results in low deviations due to noise; (ii) supernoise robustness enables superlinear scaling with the number of coupled units; (iii) the state variables are at local maxima or minima resulting in easier reading of the state variable. Recently, Blakely *et al.* [43] showed that zero derivative events are regularly timed in a topologically diverse class of chaotic oscillators. A combination of superlinear noise suppression and regular timing will enable many practical technological applications of robust coupled dynamical systems.

ACKNOWLEDGMENTS

We gratefully acknowledge support from the Office of Naval Research under Grant No. N000141-21-0026 and STTR Grant No. N00014-14-C-0033.

[1] S. H. Strogatz, *Nonlinear Dynamics and Chaos: With Applications to Physics, Biology, Chemistry, and Engineering* (Westview Press, Boulder, Colorado, 2014).
[2] B. Kosko, *Neural Networks and Fuzzy Systems: A Dynamical Systems Approach to Machine Intelligence* (Prentice-Hall, Englewood Cliffs, NJ, 1992), Vol. 1.
[3] J. Guckenheimer and P. Holmes, *Nonlinear Oscillations, Dynamical Systems, and Bifurcations of Vector Fields* (Springer Science & Business Media, New York, 1983), Vol. 42.
[4] S. Wiggins, *Introduction to Applied Nonlinear Dynamical Systems and Chaos* (Springer Science & Business Media, New York, 2003), Vol. 2.
[5] A. Garfinkel, M. Spano, W. Ditto, and J. Weiss, Science **257**, 1230 (1992).
[6] S. J. Schiff, K. Jerger, D. H. Duong, T. Chang, M. L. Spano, and W. L. Ditto, Nature (London) **370**, 615 (1994).
[7] P. A. Merolla, J. V. Arthur, R. Alvarez-Icaza, A. S. Cassidy, J. Sawada, F. Akopyan, B. L. Jackson, N. Imam, C. Guo, Y. Nakamura *et al.*, Science **345**, 668 (2014).
[8] B. Kia, J. F. Lindner, and W. L. Ditto, Front. Comput. Neurosci. **9**, 1 (2015).
[9] T. Stankovski, P. V. E. McClintock, and A. Stefanovska, Phys. Rev. X **4**, 011026 (2014).
[10] S. Sinha and W. L. Ditto, Phys. Rev. Lett. **81**, 2156 (1998).
[11] K. Murali, S. Sinha, W. L. Ditto, and A. R. Bulsara, Phys. Rev. Lett. **102**, 104101 (2009).
[12] M. Loecher, *Noise Sustained Patterns*, World Scientific Lecture Notes in Physics Vol. 70 (World Scientific, Singapore, 2003).
[13] C. W. Gardiner *et al.*, *Handbook of Stochastic Methods* (Springer, Berlin, 1985), Vol. 3.
[14] H. Risken, *Fokker-Planck Equation* (Springer, New York, 1984).
[15] N. G. Van Kampen, *Stochastic Processes in Physics and Chemistry* (Elsevier, Amsterdam, 1992), Vol. 1.
[16] I. Bashkirtseva, L. Ryashko, and E. Slepukhina, Fluct. Noise Lett. **13**, 1450004 (2014).
[17] A. Pikovsky, M. Rosenblum, and J. Kurths, *Synchronization: A Universal Concept in Nonlinear Sciences* (Cambridge University Press, Cambridge, UK, 2003), Vol. 12.
[18] S. Boccaletti, *The Synchronized Dynamics of Complex Systems* (Elsevier, Amsterdam, 2008), Vol. 6.
[19] M. Zhang, S. Shah, J. Cardenas, and M. Lipson, Phys. Rev. Lett. **115**, 163902 (2015).
[20] N. Tabareau, J.-J. Slotine, and Q.-C. Pham, PLoS Comput. Biol. **6**, e1000637 (2010).
[21] J. Bouvrie and J.-J. Slotine, Neural Comput. **23**, 2915 (2011).
[22] B. Kia, S. Kia, J. F. Lindner, S. Sinha, and W. L. Ditto, Int. J. Bifurcat. Chaos **25**, 1550040 (2015).
[23] V. Kohar, B. Kia, J. F. Lindner, and W. L. Ditto, Int. J. Bifurcat. Chaos **26**, 1650005 (2016).
[24] V. Kohar, S. Kia, B. Kia, J. F. Lindner, and W. L. Ditto, Nonlin. Dyn. **84**, 1 (2016).
[25] N. Masuda, Y. Kawamura, and H. Kori, New J. Phys. **12**, 093007 (2010).
[26] B. Kia, M. L. Spano, and W. L. Ditto, Phys. Rev. E **84**, 036207 (2011).
[27] B. Kia, S. Kia, J. F. Lindner, S. Sinha, and W. L. Ditto, Chaos **24**, 043110 (2014).
[28] T. Geisel and J. Nierwetberg, Phys. Rev. Lett. **47**, 975 (1981).
[29] G. Mayer-Kress and H. Haken, J. Stat. Phys. **26**, 149 (1981).
[30] A. Prasad, V. Mehra, and R. Ramaswamy, Phys. Rev. E **57**, 1576 (1998).
[31] M. H. Lee, J. Math. Phys. **50**, 122702 (2009).
[32] A. L. Shilnikov and N. F. Rulkov, Int. J. Bifurcat. Chaos **13**, 3325 (2003).
[33] L. Glass and J. Sun, Phys. Rev. E **50**, 5077 (1994).
[34] A. Miliotis, S. Sinha, and W. L. Ditto, Int. J. Bifurcat. Chaos **18**, 1551 (2008).
[35] Z. B. Jemaa and S. Belghith, in *Systems, Man and Cybernetics, 2002 IEEE International Conference* (IEEE, New York, 2002), Vol. 1, pp. 447–451.

[36] K. Kaneko, *Theory and Applications of Coupled Map Lattices* (John Wiley & Son Ltd., New York, 1993), Vol. 12.
[37] F. Ginelli, H. Chat, R. Livi, and A. Politi, J. Phys. A: Math. Theor. **46**, 254005 (2013).
[38] F. Ginelli, P. Poggi, A. Turchi, H. Chaté, R. Livi, and A. Politi, Phys. Rev. Lett. **99**, 130601 (2007).
[39] L. M. Pecora and T. L. Carroll, Phys. Rev. Lett. **80**, 2109 (1998).
[40] P. J. Menck, J. Heitzig, N. Marwan, and J. Kurths, Nat. Phys. **9**, 89 (2013).
[41] V. Kohar, P. Ji, A. Choudhary, S. Sinha, and J. Kurths, Phys. Rev. E **90**, 022812 (2014).
[42] L. M. Pecora, Phys. Rev. E **58**, 347 (1998).
[43] J. N. Blakely, R. M. Cooper, and N. J. Corron, Phys. Rev. E **92**, 052904 (2015).